Fast and Flexible Generation of Conductive Circuits

Philipp Amend[1], Oliver Hentschel[2,3], Christian Scheitler[2,3], Marcus Baum[2,3]
Johannes Heberle[2,3], Stephan Roth[1,3] and Michael Schmidt[1,2,3]

[1] *Bayerisches Laserzentrum GmbH, 91052 Erlangen, Germany*
[2] *University of Erlangen-Nuremberg, Chair of Photonic Technologies, 91052 Erlangen, Germany*
[3] *Erlangen Graduate School in Advanced Optical Technologies, 91052 Erlangen, Germany*

The functional and geometrical requirements to electronic, optoelectronic and mechatronic devices have significantly increased during the last years. Within the scope of the development and the fabrication of such components a very important aspect is the fast and flexible generation of conductive circuits respectively structures on work-pieces of various dimensions and materials. The presented work gives an overview about three promising laser-based approaches to generate microscopic and macroscopic circuits as well as conductive layers with a thickness in the order of a few hundred nanometers. In addition to processes for the fabrication of conductive structures laser-based soldering of piezo-composites is investigated.

DOI: 10.2961/jlmn.2013.03.0015
Keywords: conductive circuits, ITO nanoparticles, stereolithography, ADDIMID technology, Molded Interconnect Device, Laser-Beam-Melting, laser-based soldering, piezo-composites

1. Introduction and motivation

The functional and geometrical requirements for electronic, optoelectronic and mechatronic devices increased during the last years. A very important aspect in their development and fabrication is the fast and flexible generation of conductive circuits from nano to macro scale on work-pieces of various sizes and materials. The present work gives an overview about three promising laser-based approaches that can help to fulfill these requirements. Besides, connection technology plays an important role in the production of electronic components. Therefore latest results of laser-based soldering of piezo-composites are presented.

The mass production of optoelectronic devices requires flexible and inexpensive deposition methods of transparent conductive metal oxides. Alternatively to commonly used vacuum deposition methods dense metal oxide layers can be generated by deposition of nanoparticle suspensions by various printing techniques and subsequent laser consolidation. Recent publications indicate the feasibility of the process even on sensitive substrates such as polymers despite the extremely high melting temperatures of metal oxides [1, 2]. Latest results in this research field will be presented in this paper.

An innovative approach for a fast and flexible production of functional prototypes of electronic devices can be achieved for the combined use of rapid prototyping and laser - assisted selective metallization according to ADDIMID technology [3, 4].

First results using selective laser melting of polymers for the fabrication of electrical functional prototypes are already presented in [5]. In this paper the latest results for the combination of stereolithography (SLA) and ADDIMID technology will be given.

Laser-based additive manufacturing technologies such as Laser-Beam Melting (LBM) and Laser Metal Deposition (LMD) afford an opportunity for the direct, flexible and fast generation of conductive structures on comparatively widespread work pieces. By the use of LBM or LMD simple conductive lines as well as two- and three-dimensional electronic elements/structures such as electrodes or metallic sensors could be directly fabricated by laser-based processing of metallic powder without additional steps of pre- and post-processing such as chemical metallization and/or galvanic amplification. For preliminary tests a LBM-machine was used in order to investigate the feasibility of generating simple conductive lines of pure aluminum on sheet metals coated with a thin polyamide 12 (PA 12) layer. Within the scope of this paper latest results of this research will be presented.

For applications requiring both a strong mechanical and electrical connection, laser soldering can be applied. The main challenge of such a thermal process is to prevent high temperatures above the Curie temperature (T_c = 120 °C - 330 °C) to the piezoceramic to keep the piezoelectric effect. To limit the heat transfer only to diffusion the solder preform is melted in a nozzle by a laser beam and deposited between two piezoceramic plates. In this paper the latest results for the production of these piezoceramic composite modules are presented.

2. Functional Principles and Experimental Setup

2.1 Laser Treatment of nanoparticle suspensions

In the presented experiments, ITO nanoparticles commercially available from Evonik Industries AG, with a primary particle size of about 20 nm and a particle size distribution ranging from 20 nm to 120 nm are used. The particles were dispersed in ethanol at a 20 wt% loading while a particle agglomeration in the suspensions was prevented by addition of trioxydecanoic acid, which works as a steric stabilizer. The production of the suspensions is described in detail in [6]. In order to generate ITO particle layers by spin coating, portions of 200 µl of the suspension were deposited on 25 mm × 25 mm × 1 mm soda lime substrates and spun at 3000 rpm for 20 s. The layer thickness was adjusted by dilution of the suspensions with additional ethanol prior to the deposition. After deposition the samples were thermally annealed on a hot plate for 30 minutes in ambient air at 450 °C. At this temperature the stabilizing agent is oxidized and completely removed from the particle layer while no major morphological changes such as sintering among adjacent particles are caused according to SEM analysis. For the laser consolidation of the particle layers, a Lambda Physik LPX 315i KrF Excimer laser with a wavelength of 248 nm and a pulse length of about 30 ns, a maximum pulse energy of 0.8 J, a maximum average power of 75 W, and a raw beam size of 15 mm × 30 mm was used. The raw beam was limited to a size of 5 mm × 30 mm by an aperture in order to cut off the inhomogeneous regions at the borders of the beam. Analysis of the surface morphology and cross-sections of the ITO films was conducted by SEM (JEOL, 7500F). The film thickness was determined by introducing scratches on the sample surface and measuring several height profiles of these scratches with a laser scanning microscope (Olympus Lext OLS4000). The sheet resistances of the prepared films after the deposition and different treatment steps were measured by a Keithley multimeter in a linear 4-point setup with an equidistant electrode separation of 1 mm.

2.2 Stereolithography and ADDIMID technology

A 3D Molded Interconnect Devices (MID) is an injection-molded plastic part that combines electrical and mechanical functionalities with integrated conductive circuits in a single assembly [7]. In the last years functional and geometrical requirements for MID have been increased [8]. Therefore functional MID prototypes for an economic and efficient product engineering during the conception stage are essential [9]. However using current MID technologies to fabricate geometrical complex prototypes is expensive and highly time-consuming because expensive injection molds are needed [10]. A fast and flexible production of complex 3D MID prototypes can be achieved by the use of stereolithography (SLA).

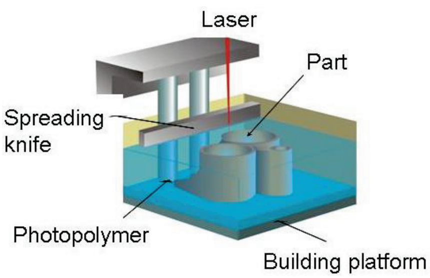

Fig. 1: Functional principle of stereolithography

The prototypes are produced directly from CAD data without the use of any shape forming tools. The selective curing of the SLA resin is realized by a UV laser ($\lambda = 355$ nm). The UV laser radiation causes an activation of the light sensitive initiators that are contained in the resin. The electrical functionality of the fabricated devices is realized by a laser structuring process with a pulsed ns-IR-laser (see Fig. 2). Therefore the used stereolithography material NanoTool is doped with aluminum metal fine powder (AS MEP 027, ECKA Granulate GmbH & Co. KG). The metal particles in the fabricated SLA parts absorb the laser radiation and heat the polymer matrix up to its ablation threshold. This physical thermal reaction leads to a surface activation of the SLA part and the exposed metal acts as catalytic nucleation site. The conductive circuits are formed by chemical metallization (Enthone LDS Cu-9070).

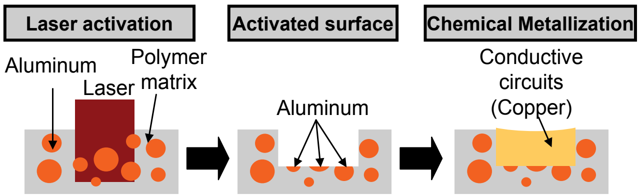

Fig. 2: Process chain of ADDIMID technology

To analyze the influence of aluminum on the laser-based photopolymerization specimens according to the WINDOW PANE methode [11] are fabricated. The specimens consist of five measurement areas and a frame structure. Each of the rectangular areas is fabricated through a single layer exposure. The variation of the velocity from 10 to 1000 mm/s leads to different curing depth C_D.

After that, the mechanical properties of aluminum doped SLA parts are characterized by means of tensile tests. Additionally, the adhesion of the metallization is analyzed by means of cross-cut testing. For the evaluation of the cross-cut test a rating scale from GT0 to GT5 is used. Thereby GT0 describes very good adhesion and GT5 very bad adhesion. To determine the adhesion between metallization and electrical components shear tests are performed. The electrical components (0603, zero ohm resistor) are joint by means of condensation soldering (Sn96.5 Ag3 Cu0.5). With regard to serial production, basic reliability aspects are assessed. Therefore, temperature shock tests (-40 °C / +125 °C) are performed. The resistance is measured before the climate test as well as after 500 and 1000 cycles of the temperature shock test.

2.3 Laser-Beam-Melting of conductive circuits

Within the scope of these experiments a commercially available argon-atomized aluminum powder with a purity of 99.9 % and an approximately spherical particle shape from TLS Technik GmbH & Co. Spezialpulver KG was used. Prior to the experiments the powder was sieved and thermal treated for 3 hours in a furnace under argon-atmosphere at a temperature of 100 °C to improve the powder flowability in order to achieve homogeneous powder layers during the recoating process. After sieving the applied aluminum particles possessed mainly particle-diameters between 40 µm and 50 µm and the proportion of smaller particles was significantly minimized. If the particle size of the aluminum powder was selected smaller than 40 µm, the aluminum powder showed an enhanced formation of agglomerates, whereby the grade of agglomerate formation enhanced with decreasing particle diameter.

For implementing the experiments two different kinds of plastic coated aluminum sheet metal samples were devoted. In both cases the basic polymer was polyamide 12 (PA12), whereby half of the samples were doped with carbon black particles to enhance laser light absorption. The thickness of the coatings conformed to approximately 300 µm and the adhesion between the plastic coating and the aluminum sheet metal was achieved by a thin adhesion agent layer with a thickness of 10 µm.

To analyze the feasibility of the direct fabrication of conducting paths on plastic coated sheet metals a LBM-machine - ReaLizer SLM 50 - was used. In Fig. 3 the setup of the LBM-machine is schematically displayed.

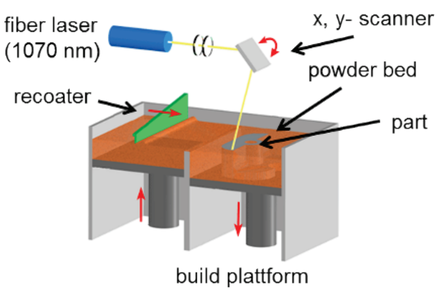

Fig. 3: Principle of a LBM-machine setup [12]

As laser source a cw-single-mode fiber laser with high beam quality ($M^2 < 1.1$) and a wavelength of 1070 nm was applied. The laser power was varied between 20 W and the maximum of 100 W. The laser beam was guided by a galvanometer-scanner in x- and y- direction and focused on the substrate by an F-Theta objective. According to the machine manufacturer the spot diameter of the focused beam conforms to roughly 10 µm.

The successive proceeding within the scope of the experiments is schematically illustrated in Fig. 4. In a first process step a thin powder layer with a layer thickness in the order between 30 µm and 300 µm was deposited on the plastic coated sheet metal sample by the recoating mechanism of the SLM 50. Subsequently to the powder deposition these layers were locally irradiated. Prior to the selective irradiation of the pre-placed aluminum powder the scanning strategy was determined and programmed in MagicsRP.

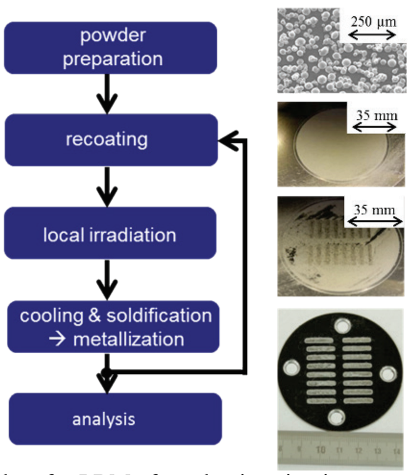

Fig. 4: Procedure for LBM of conductive circuits

In addition to thin, simple metallic lines larger metallic line-structures were fabricated on the PA12 coatings by placing lines next to each other and stacking these on top of each other. In this context different multi line/layer strategies were investigated in order to generate solid, conductive aluminum lines.

Depending on the selection of process parameters such as laser power P, powder layer thickness d, Point-to-Point distance PTP, exposure time ET and the applied process-respectively irradiation strategy metallic lines with partly good bonding to the insulating plastic surface and at least partially electrical conductivity have been fabricated without destroying the PA12 coating as consequence of energy respectively heat input. The analysis of the generated solid aluminum lines was done by metallographic preparation of the samples and the subsequent microscopy of the conductive lines and the grindings along and perpendicular to the scanning direction. Furthermore the substrate bonding was proved manually by simple scratch tests with a kind of a metallic spike. To verify the electrical conductivity simple resistance measurements were conducted with a conventional ohmmeter.

2.4 Laser-based soldering of piezo-composites

It has been shown that parallel arrangement of piezoceramic rods is ideal for direct integration of piezoelectric transducers into laminar structures [13]. To produce such structures prefabricated stacks made of monolithic PZT wafer or PZT-fiber-composite plates with removable elastomeric spacers between each pair of plates (Fig. 5) can be used. The monolithic piezoceramics (VIBRIT 1100) were purchased from Johnson Matthey Piezoproducts and the composites were produced by fiber spinning and casting of epoxy resin [14]. The spacers and the plates have both a thickness of 250 µm resulting in a gap of the same size at each end of the stack. The gaps have to be filled with solder and by dicing this stack subsequentially an arbitrary number of electrically and mechanically bonded rods can be achieved in one cut [15].

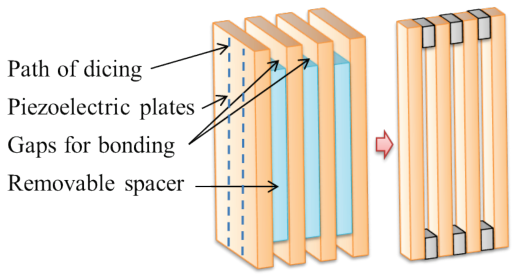

Fig. 5: Prefabricated stack of piezoceramic wafers and final state of the piezoceramic composite stack

To investigate the generation of the electrodes in this paper a SB² remote device (Pac Tech Inc.) was used. The principle of the experimental setup is shown in Fig. 6.

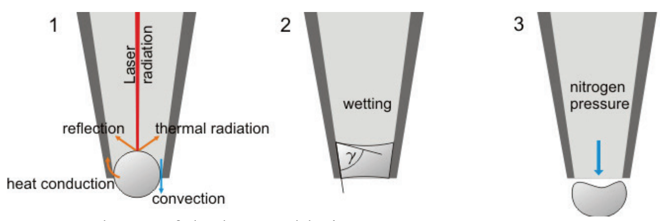

Fig. 6: Scheme of the laser soldering process

A solder preform (Sn95.5Ag4Cu) is fed into a WC/Co nozzle and blocks the outlet. The diameter of the preform and the nozzle can be varied between d = 200 µm and d = 600 µm. The Yb:YAG fiber laser at wavelength λ = 1070 nm and a maximum power P = 30 W is focused coaxial by a convex lens with focal length f = 45 mm on the solder preform. During a single laser pulse the solder ball is melted and wets the metallic nozzle. Nitrogen pressure has to be applied to push out the solder and to position it by this in the gap between the piezoelectric substrates. As the gap is much longer than the solder preform multiple solder preforms have to be positioned next to each other by moving the nozzle along the gap. The introduced heat is kept at a minimum and transferred only by diffusion from the molten solder. Thereby, direct heating of the sensitive material is avoided.

3. Experimental results

3.1 Laser Treatment of nanoparticle suspensions

ITO particle layers were generated on soda lime substrates by spin coating of the particle dispersions. The layers display a thickness of 440 nm ± 20 nm. In order to adjust the layer thickness a series of different dilution levels was prepared by adding increasing amounts of pure ethanol to the initial particle suspension. The obtained layer thicknesses are shown in Fig. 7. They are in good agreement with the layer thicknesses expected based on the level of dilution.

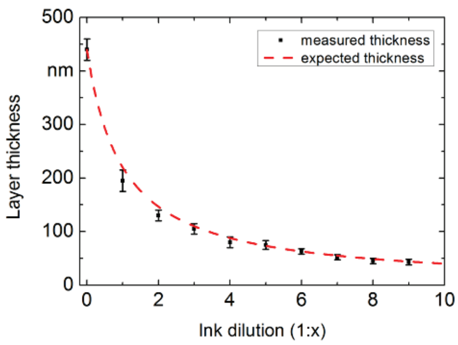

Fig. 7: Layer thicknesses obtained by dilution of the initial suspension in a ratio of 1:x as well as the expected layer thickness d which is estimated by $d = d_{undiluted}/(1+x)$

The created particle layers initially have a very high sheet resistance which is in the order of 1 MΩ even for the thickest layers produced due to particle-particle separation by the steric stabilizer contained in the suspension. After removal of the stabilizing agents by thermal annealing at 450 °C on a hot plate for 30 minutes particle contact is enabled resulting in a significant decrease of the observed sheet resistance. For 440 nm thick layers the sheet resistance drops to 2700 Ω ± 300 Ω which corresponds to a layer conductivity of about 8 S/cm ± 1 S/cm. The measured value for the conductivity stays constant for all layer thicknesses produced within the accuracy of the measurements and does not show any unexpected behavior. In order to increase the layer conductivity, annealed particle layers of different thicknesses were irradiated by single Excimer laser pulses with the aim of layer consolidation and increase of the particle-particle contact area. The laser wavelength of 248 nm used in the experiments is efficiently absorbed in ITO due to interband absorption which leads to a penetration depth as low as 50 nm in bulk ITO [16]. Fig. 8 shows the effect of laser irradiation for an exemplary particle layer. A significant layer consolidation at the top of the particle layer down to a depth of about 50 nm where almost full density is reached is observed in the cross-section image.

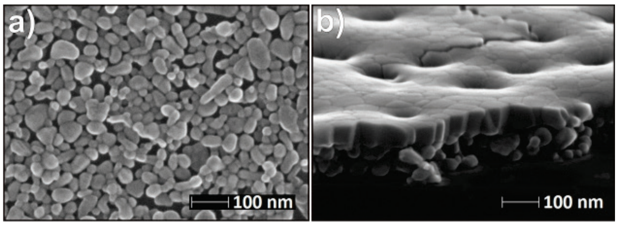

Fig. 8: a) SEM image of an exemplary particle layer after annealing prior to laser irradiation (top view); b) SEM image of an exemplary particle layer cross-section after laser irradiation with a single laser pulse

Experiments for different layer thicknesses between 55 nm and 440 nm for laser fluences ranging from 20 mJ/cm² to 160 mJ/cm² were carried out. The results of the experiments for a layer thickness of 195 nm ± 10 nm as well as a layer thickness of 55 nm ± 5 nm are shown in Fig. 9 a) and b).

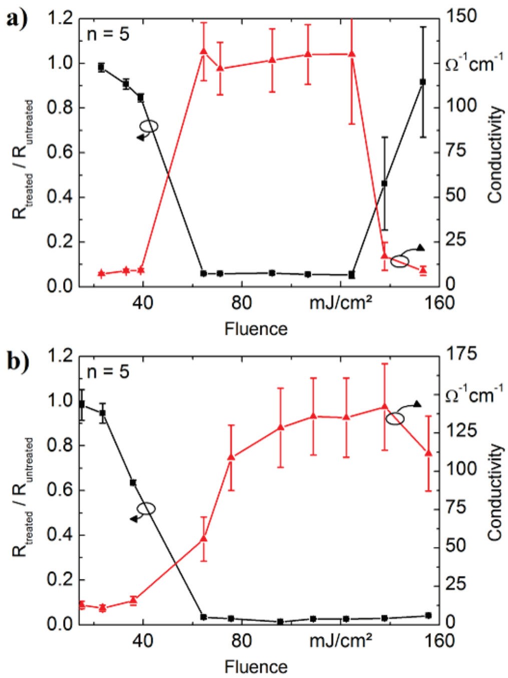

Fig. 9: Changes in the sheet resistance of the particle layers (a) 195 nm ± 10 nm b) 55 nm ± 5 nm) after laser treatment with respect to their initial value ($R_{treated}/R_{untreated}$, black curve, squares) for different laser fluences as well as their absolute conductivity (red curve, triangles)

While fluences below 30 mJ/cm² do not lead to major changes in the layer resistance, starting at fluences of about 40 mJ/cm² noticeable changes are observed. Significant decrease in the sheet resistance and increase in the layer conductivity are observed for fluences of about 60 mJ/cm² and more indicating major structural changes in the layer morphology. While the maximum conductivity is reached at about 60 mJ/cm² for the 195 nm thick layer, higher fluences are needed when the layer thickness is decreased to 55 nm. This is likely to be a consequence of a lower energy input due to the lower thickness of the layer. At the same time the transfer of thermal energy from the layer towards the substrate is expected to be higher for thinner layers as the hot areas are in direct contact with the substrate. For fluences above 120 mJ/cm² the sheet resistance displays an upturn for the 195 nm thick layers, while the films are turning milky and display irregular conductivity properties indicating cracks and ablation of the layer. The same behavior is also starting to emerge for the thinner layer for slightly higher fluences. Furthermore the thinner layer shows a higher total conductivity in comparison to the thicker one. This becomes especially apparent if the maximum conductivities, which were reached for different layers, are compared with respect to the layer thickness (see Fig. 10).

Increasing conductivities are observed for decreasing layer thicknesses indicating inhomogeneous conduction through the layer cross-section. For the layers below 100 nm in thickness the conductivity appears to reach its maximum. This behavior becomes plausible when taking into account that only approximately 50 nm at the top of the particle layer will reach full density during laser consolidation while the morphology of the underlying particles is almost unchanged. Consequently a higher conductivity at the layer surface can be expected. As the consolidated region of the layer is expected to be more or less independent of the layer thickness, the maximal conductivity is expected to be found for thin layers.

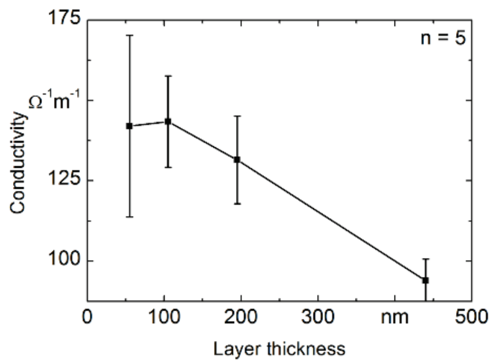

Fig. 10: Maximum ITO layer conductivities for different layer thicknesses

3.2 Stereolithography and ADDIMID technology

To characterize the UV curing behavior of the filled stereolithography resin the curing depths CD for different weight contents of aluminum are determined. Besides the curing depth for unfilled resin is measured. In this case NanoTool that can be purchased from DSM Somos and has no additionally aluminum fillers is declared as unfilled resin even if this material itself is highly filled with non-crystalline nanoparticles. Fig. 11 shows the results of the performed measurements. It is clear that the curing depth decreases with increasing aluminum content for a constant energy density. For unfilled resin the curing depth is influenced by the nanoparticles and the resin. For aluminum filled resins there is an additional laser-material interaction between the aluminum particles and the UV laser radiation. On one hand, the laser radiation is absorbed by the aluminum particles and the other hand, the radiation is reflected on the particle surface. Typically aluminum has a low absorption and a high reflectivity. However the additionally absorbing material leads to a decrease of curing depth and hence to a lower penetration depth of the laser radiation. This means that a higher energy density is required for the filled resin in comparison to the unfilled resin to achieve the same curing depth. However the experiments show that the functionalized resin systems can be cured despite additional aluminum fillers. This leads to the conclusion that these new materials are suitable for the SLA process.

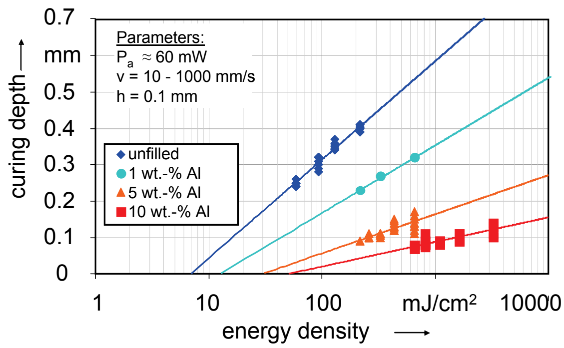

Fig. 11: Working curves according to the WINDOW PANE method for NanoTool with different aluminum contents

To characterize the mechanical properties of the new material tensile bars are manufactured on a SLA 250/50 (3D Systems). Therefore NanoTool + 1 wt.-% Al is used as resin. The performed tensile tests for aluminum filled specimens provide an average tensile strengths of 77.1 MPa ± 8.9 MPa. The manufacturer of NanoTool specifies the tensile strength of the material with 61.7 MPa to 80.3 MPa depending on the post processing (only UV curing: 61.7 MPa to 78 MPa; UV and thermal postcure: 66.3 to 80.3 MPa [17]. This fact leads to the conclusion that the mechanical properties are not significantly influenced by 1 wt.-% aluminum.

A good adhesion between the metallization and the substrate is of great importance for functional conductive circuits. To characterize the adhesion of the metallization cross-cut tests are carried out. Fig. 12 (left side) shows an example of a metallization after the cross-cut test.

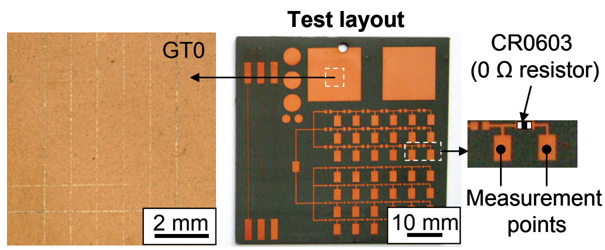

Fig. 12: Test layout with areas for cross-cut test and resistance measurement

The evaluation of the cross-cut test leads to the conclusion that the adhesion between the metallization and the SLA substrate is very good (GT0). The cut edges are completely smooth and none of the squares in the grid is chipped. The cross-cut test is performed on five samples. The analysis shows always a good to very good adhesion, so that a reproducible metallization with high quality can be assumed.

The results for the resistance measurement shown in Fig. 13 refer to the setup in Fig. 12. Therefore a zero ohm component is soldered on a conductive circuit (conductor width: 300 µm, conductor height: about 6-8 µm) and the resistance is measured with an ohmmeter. The determined resistances show nearly constant values in the range of 0.14 Ω to 0.16 Ω independent of the aging of the samples by means of climate tests (see Fig. 13). However the shear forces to remove the electrical component increase with growing amount of cycles.

For unaged samples, almost always a fracture between substrate and metallization occurs. After 500 cycles more often a failure of the solder joint or at the interface between the solder and the metallization take place. This trend continues for specimens tested after 1,000 cycles. The temperature changes during the climate tests lead to a superposition of thermal and mechanical stress which causes a shear strain in the solder. In addition, soft solders like Sn96.5 Ag3 Cu0.5 tend to creep due to temperature changes [18]. The enumerated types of load can be mentioned as cause for the failure of the solder after the climate tests. The realized shear forces of the soldered components are sufficient for MID prototypes.

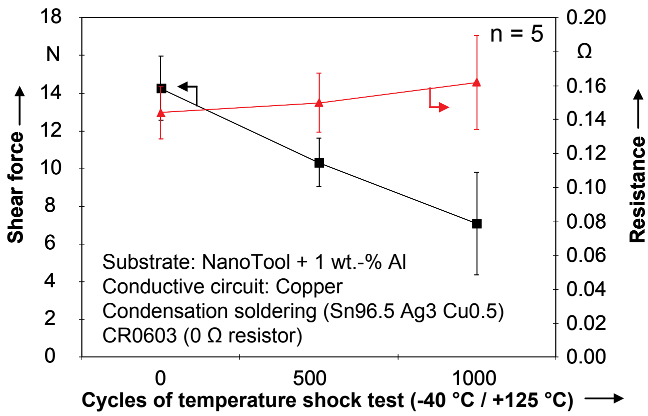

Fig. 13: Shear force and resistance of electrical components (0603, zero ohm resistor) before and after temperature shock test

The use of stereolithography (SLA) enables a fast and flexible fabrication of complex 3D prototypes. However, only the combination of SLA and ADDIMID technology allows the realization of electrical functionalized 3D MID prototypes. The evaluation of the experiments show that the aluminum doped resin can be used for SLA and the mechanical properties of the fabricated specimens are comparable to unfilled NanoTool. The analysis of the metallization quality by means of cross-cut testing demonstrates that the adhesion between the metallization and the SLA substrate is very good. Even the realized resistance of the conductor circuits before and after aging caused by climate tests is very low. The shear force which is necessary to remove the soldered electrical component is influenced by the climate test. However the reached values are acceptable for functional prototypes. All in all the proposed approach is a suitable solution for manufacturing 3D MID prototypes by means of SLA and ADDIMID technology.

3.3 Laser-Beam-Melting of conductive circuits

As mentioned previously the layer thickness of the deposited aluminum powder is an important process parameter. Within the scope of these experiments the ideal layer thickness conforms to about 100 µm is analyzed. In this instance nearly homogeneous powder layers could be deposited and after laser processing with convenient process parameters sufficient metallization on the plastic surface was achieved without destroying the coatings.

If the layer thickness was selected smaller than 100 µm, no homogeneous powder layer could be deposited. In this case a large fraction of the plastic surface was uncoated and therefore it was not possible to generate continuous conductive lines. Additionally, if the layer thickness was too thin, an enhanced direct laser energy input caused a strong heating up of the irradiated plastic volume to temperatures above the decomposition temperature of PA12. As consequence of this ablation of the PA12 layer was the dominant effect.

If the layer thickness was selected smaller than 100 µm, no homogeneous powder layer could be deposited. In this case a large fraction of the plastic surface was uncoated and therefore it was not possible to generate continuous conductive lines. Additionally, if the layer thickness was too thin, an enhanced direct laser energy input caused a strong heating up of the irradiated plastic volume to temperatures above the decomposition temperature of PA12. As consequence of this ablation of the PA12 layer was the dominant effect.

Experiments completed with a layer thickness in the order of 150 µm and larger have shown, that no sufficient metallization was achievable, as the energy transfer into the plastic layer was presumably not intensive enough to achieve surface modification and bonding between the metal particles and the plastic surface. Based on these findings the ideal layer thickness was determined to 100 µm and kept constant for the subsequent presented experiments.

Another important process parameter was the Point-to-Point distance PTP. As shown by analysis based on variation of the PTP a statistical, but approximately homogeneous metallization along and perpendicular to the scanning direction was observed for PTP values of less or equal 20 µm. When the PTP distance was increased to 30 µm or up to 50 µm the absorbed energy along a single scanning line became more and more inhomogeneous. As a consequence just punctual metallization and no homogeneous metallization along to the scanning direction were observed. Because of this the PTP distance was kept constant at 10 µm for the further presented experiments.

In addition to the laser power and the Point-to-Point distance the exposure time ET is a fundamental process parameter. An increase of ET is equivalent to a decrease of the averaged scanning velocity v, which results in an increase of the averaged line energy E_{line} under the assumption of constant laser power and PTP distance.

As displayed in Fig. 14 a) statistical, but approximately homogeneous metallization along and perpendicular to the scanning direction could be already achieved on the carbon black doped PA12 coatings with a low exposure time of

20 µs and a laser power of 50 W, which corresponds to an averaged line-energy E_{line} of 0.1 J/mm. The rate of metallization was intensified with increasing laser power. The widths of the generated linear metallization tracks averaged more than 200 µm, which is at least 20 times larger than the laser spot diameter of about 10 µm.

Probably the large width of the metallization tracks was a consequence of heat conduction in a plane parallel to the layer surface causing a comparatively widespread melting of the plastic surface ($\lambda_{Al,\ bulk}$ = 236 W/(m K) [19], $\lambda_{PA12,\ undoped}$ = 0,23 W/(m K) [20]. The deposited aluminum particles were bonded to the plastic coating by form closure respectively a mechanical fixing. In Fig. 14 b) a SEM-image of a generated linear metallization track is displayed, that shows the form closure between the PA12 coated surface and deposited aluminum particles. The molten plastic was flowing around the pre-placed aluminum particles and solidified after cooling down. The result of this form closure was a strong bonding between the deposited particles and the PA12 layer that was proved by applying scratching tests with a metallic spike on the surfaces. As shown in Fig. 14 c), the bonded particles were only partly fused respectively sintered together, so that no electrical conductivity could be verified by simple resistance measurements at this state.

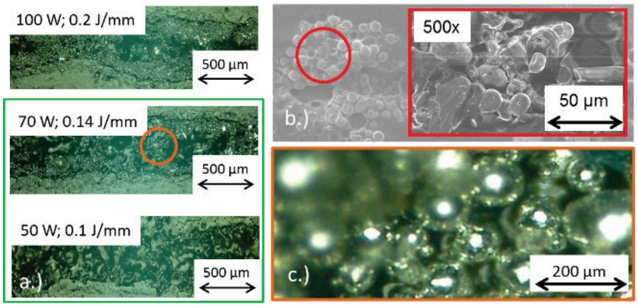

Fig. 14: a) Fabricated linear aluminum tracks for a constant exposure time ET of 20 µs and different values of laser power; b) SEM-Image of a generated linear metallization track illustrating the form closure between the deposited Al-particles and the PA12 surface; c) Partially fused respectively sintered Al-particles

With an increase of the exposure time ET the rate of metallization in the middle of the scanning line decreased more and more. This context is illustrated in Fig. 15 for exposure times of 40 µs and 80 µs and varying laser power.

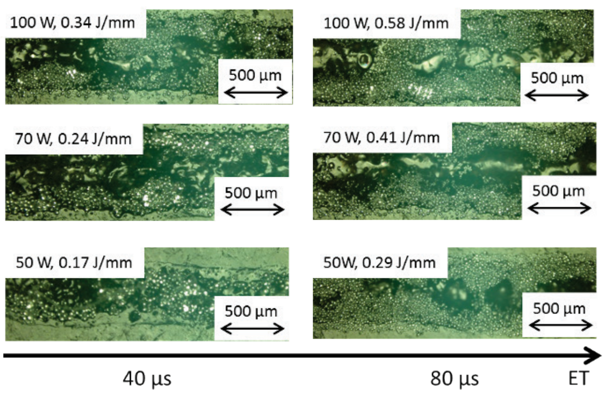

Fig. 15: Fig.4: Fabricated linear, non-conductive aluminum tracks for an exposure time ET of 40 µs and 80 µs and different values of laser power.

If the averaged line energy E_{line} reached values up to approximately 0.2 J/mm and larger, the carbon black doped PA12 layer was strongly heated up by direct laser light absorption and heat conduction with the irradiated aluminum particles. Resulting of the large heat input the doped PA12 reached temperatures over its decomposition temperature and hence material-ablation was the observed dominating effect. As a function of the applied laser power and the selected exposure time the observed ablation of the carbon black doped PA12 layer was so strong, that more than 2/3 of the layer thickness was ablated by single line scanning. Consequently the biggest proportion of the deposited metal particles was removed from the processing zone. In contrast to the middle section of a single scanning line a strong metallization could be observed at the edges of the formed ablation tracks as consequence of heat conduction, melting and subsequent form closure.

In contrast to the rate of metallization, which could be achieved on the carbon black doped PA12 coatings the amount of bonded aluminum particles on the undoped PA12 coatings was comparatively less. The lower rate of metallization was the result of mainly two effects, whereby its appearance was depended on the magnitude of averaged line energy E_{line}. In the case of a line energy E_{line} less or equal to 0.3 J/mm the observed surface near melting was not sufficient to bond the pre-placed Al-particles by form closure with the plastic surface as consequence of the poor laser light absorption compared to the laser light absorption of the carbon black doped PA12 coatings. In the range of low line energy E_{line} no permanent metallization of the untreated PA12 coatings was achievable.

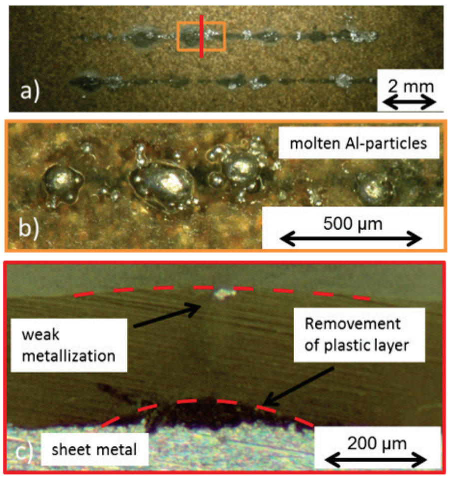

Fig. 16: a) Achieved inhomogeneous metallization on untreated PA12 coating (E_{line} = 0.6 J/mm), b) remaining, molten Al-particles (E_{line} = 0.6 J/mm), c) removal of PA12 coating and surface-near deformation of the PA12 coating (E_{line} = 0.6 J/mm)

As shown in Fig. 16 a) poor and inhomogeneous metallization of the untreated PA12 coatings along the scanning direction occurred, when the averaged line energy E_{line} was increased up to 0.6 J/mm. But in this case the remaining aluminum was completely molten and strongly bonded to the plastic surface, as can be seen from Fig. 16 b.). In this range the resulting poor metallization is also indirect a consequence of the poor laser light absorption and the involved large optical penetration depth of the laser light into the untreated PA12 coatings. Most of the laser light reached the boundary between the placed powder layer and the plastic coating transmitted through the plastic and was absorbed by the thin Co-polyamide, adhesion agent layer and the aluminum sheet metal. As consequence of the light absorption the thin layer was heated up and began to extend in order that the bonding between the sheet metal and the plastic layer was attenuated. The expansion of the heated up adhesion agent layer caused the removal of the untreated PA12 coating and a surface-near deformation. Because of these deposited and bonded metal particles were probably removed from the surface, so that the resulting metallization was inhomogeneous along the scanning line. The deformation of the surface and the removal of the plastic coating are illustrated in Fig. 16 c) for an averaged line energy E_{line} of 0.6 J/mm.

Another reason that is independent on the poor laser light absorption, for the achieved poor and inhomogeneous metallization compared to the experiments with the sheet metal samples coated with doped PA12 layers could be the absence of carbon black particles. It can be assumed that the carbon black particles operate as nucleus supporting and simplifying the adhesion respectively bonding of metallic particles to the surface. But this is only an assumption and has to be investigated in detail within the scope of future research activities.

Concluding it can be summarized that conductive circuits of pure aluminum could not be directly fabricated on a sheet metal coated with a thin PA12 layer by single layer/line experiments. However in the case of the carbon black doped PA12 layers, it was possible to generate approximately homogeneous, strongly bonded, but non-conductive linear metallization tracks by applying convenient process parameters.

For the stated reasons further experiments, based on multi-line/layer strategies and the defined variation of the averaged line energy E_{line}, were implemented in order to investigate the feasibility of generating conductive lines on sheet metals coated with carbon black doped PA12 layers by LBM.

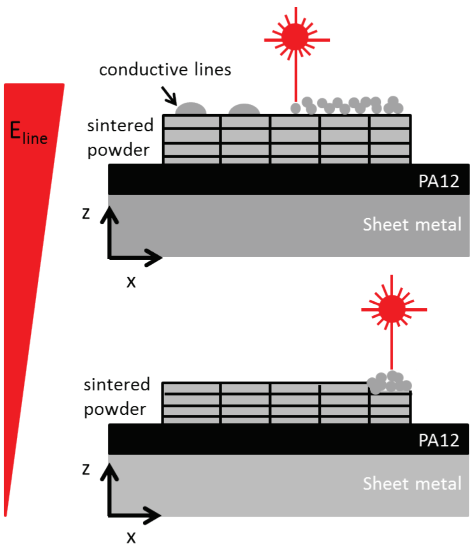

Fig. 17: Schematically display of the procedure within the scope of the multi-line/layer experiments on sheet metals coated with carbon black doped PA12 layers ($T_{Al,\ melting}$ = 660 °C [19], $T_{PA12,\ melting}$ = 178 °C [20])

Within the scope of the multi-line/layer experiments the rate of metallization was initially enhanced by placing several metallization tracks closely side by side and repeating this procedure for several layers recoated and irradiated by the laser beam successively. After the recoating of a last layer the applied averaged line energy E_{line} was increased by increasing the exposure time ET and/or laser power P in order to re-melt bonded and new deposited particles (metallization). Hereby solid aluminum lines with measurable electrical conductivity and a sufficient bonding to the plastic coating should be generated. The procedure of these multi line /layer experiments is schematically displayed in Fig. 17.

In Fig. 18 three linear metallization tracks, generated by applying the above described process strategy, are displayed for a laser power of 50 W, 70 W and 100 W. The distance between two parallel scanning lines - the so-called hatch distance h - conformed for the three shown metallization tracks to 400 µm. Furthermore the exposure time was kept constant at 20 µs. In total four powder layers with a layer thickness of 100 µm were deposited, whereby each powder layer was irradiated with five lines.

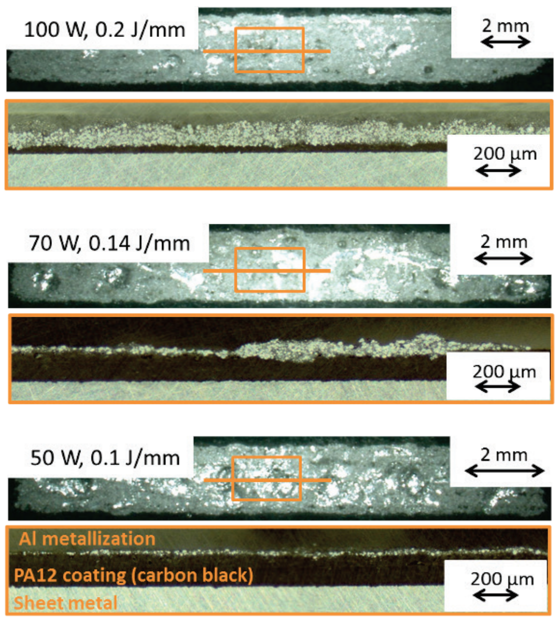

Fig. 18: Enhancement of the rate of metallization by depositing 4 layers, whereby each powder layer was irradiated with five lines of 50 W, 70 W and 100 W and a constant exposure time of 20 µs

Independent on the averaged line energy E_{line} aluminum tracks with a width in the order of nearly 3 mm could be generated. All of the fabricated metallization tracks possessed a statistical, but dense and homogeneous distribution of bonded aluminum particles along and perpendicular to the laser scanning direction. The bonded metal particles were not completely molten and hence no electrical conductivity could be measured during subsequent analysis.

Furthermore the bonding to the plastic coating was very strong in order that no removal of the metallization could be observed after conducting simple scratching tests.

Moreover it could be recognized that with an increase of the laser power respectively the averaged deposited line energy E_{line}, the rate of metallization reinforced constantly. However an increase of the averaged line energy E_{line} caused a reduction of the plastic layer thickness, as can be seen from Fig. 18.

As already mentioned previously conductive aluminum lines should now be generated by enhancement of the averaged line energy in order to guarantee fusion of the powder particles.

Therefore, after the deposition of the fifth and last powder layer the line energy E_{line} was enhanced. According to the explained experimental method several experiments were conducted by increasing the exposure time ET and the laser power P. After fabrication and cleaning a scratch test was conducted to analyze the bonding of the solid aluminum lines to the substrate. First results of these experiments are displayed in Fig. 19. In this context the averaged line energy E_{line} was enhanced from 0.1 J/mm to approximately 0.25 J/mm for the irradiation of the fifth layer and five solid aluminum lines with a hatch distance of 400 µm were generated.

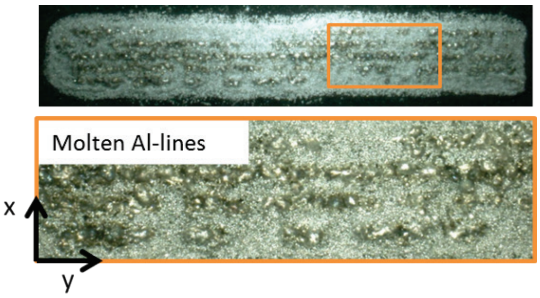

Fig. 19: Fabricated conductive solid aluminum lines (P = 70 W, ET = 40 µs, E_{line} = 0.25 J/mm) after implementation of scratching tests

As can be seen from Fig. 19 large sections of the generated conductive lines were removed by applying scratching tests. But the remaining metallization of the lines were strongly bonded to the plastic coating and could not be removed by carrying out scratch tests on the surface. Of greater scientific importance is the fact that the remaining sections of these lines were nearly completely molten and possessed electrical conductivity, which was proven by simple electric resistance measurements.

Based on these findings it was tried to fabricate solid aluminum lines of larger widths by decreasing the hatch distance between single scanning lines. In this context the hatch distance was reduced from 400 µm to 100 µm and the averaged line energy corresponded to 0.25 J/mm. In Fig. 20 a) and b) conductive lines generated in this way are shown.

As can be seen from Fig. 20 c) and d) the deposited particles were nearly completely melted down. As consequence electrical conductivity could be proved for each of the conductive lines illustrated in Fig. 21 by simple resistance measurements between its ends. Although the conductive lines were all generated by applying the same process strategy and equal process parameters a strong fluctuation of the measured resistances was observed, whereby the values varied between 0.3 Ω and 1.3 Ω. Furthermore a large proportion of the fabrication conductive lines could be removed by carrying out scratch tests at the surfaces.

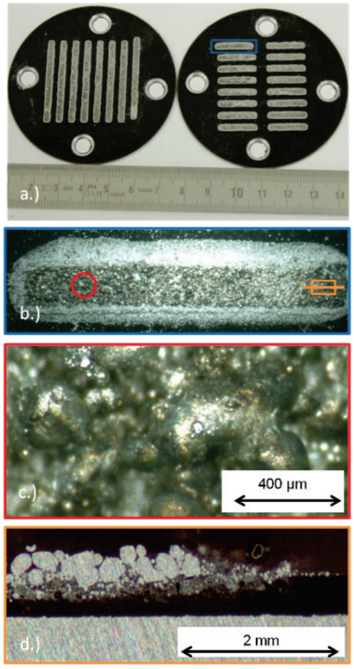

Fig. 20: a) Fabricated conductive solid aluminum lines with a width of 3 mm and different length (P = 70 W, ET = 40 µs, E_{line} = 0.25 J/mm, hatch = 100 µm); b) solid aluminum line with a width of 3 mm and a length of 14 mm (P = 70 W, ET = 40 µs, E_{line} = 0.25 J/mm, hatch = 100 µm), c) molten Al-particles; d) cross-section of the fabricated line along the scanning direction

3.4 Laser soldering for electrical and mechanical interconnection

To investigate the best conditions for a connection of two piezoelectric parts a variation of the process parameters (laser power P, pulse duration t_p, nitrogen pressure p, nozzle distance from the substrate h and the solder size d) was carried out.

To fill the gap between the two parts high positioning precision is required, as the gap width is on the order of the solder size. Previous experiments showed that asymmetric detachment can occur [21]. Also a high velocity of the solder preform leads to repulsion from the piezoceramic due to the high surface tension of the liquid solder. As the wetting of the metallization is time dependent the solder ball cannot build up adhesive forces and bounces off. Therefore, the distance from the substrate is kept at h=0.5 mm. From the same reason the nitrogen pressure is remained constant at p=20 mbar which is the minimal value for ensured detachment of the solder preform from the nozzle.

The two tested sizes of the solder preforms represent two different processing strategies which were examined. The larger preforms (d = 0.6 mm) are positioned onto the gap (d_g = 0.24 mm) and fill it due to the wetting of the surface and capillary forces. The small preforms (d = 0.2 mm) can be brought in directly into the gap. Both methods were performed successfully, however, larger preforms are more advantageous with respect to mass production. Faster processing is possible and the gap is filled more completely as can be seen in Fig. 21.

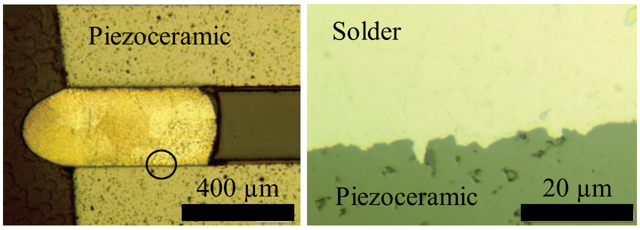

Fig. 21: Micrographs of a solder connection between two piezoceramics

To melt the solder single laser pulses with a pulse duration $t_p = 80$ ms and a laser power of $P = 30$ W were applied. The resulting pulse energy of $E = 2.4$ J is sufficient for complete melting, detachment from the nozzle and wetting of the metallized piezoceramic surface. As the piezoceramic is already polarized and the melting temperature of the solder (T_m= 223 °C) is higher than the Curie temperature of piezoceramic (T_c = 177 °C), the piezoelectric function can be impaired. Therefore, we investigate the temperature distribution by a numerical simulation of the heat diffusion from the solder located in a gap between two PZT-plates for a time duration of $t = 100$ ms, including heat contribution from the previous solder sequence and cooling of the surface by the nitrogen jet from the nozzle. The laser pulse energy influencing the temperature of the molten solder material, is considered by a variation of the initial temperature (T_i = 230 - 350 °C) of it. The layer thickness L which exceeds the Curie temperature can be seen in Fig. 22.

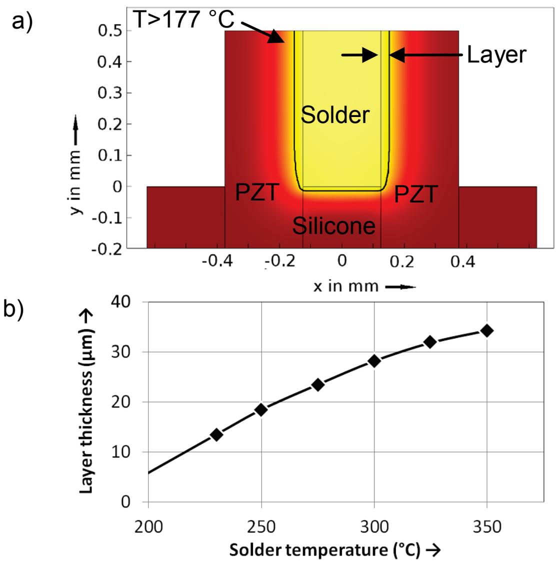

Fig. 22: a) Numerical simulation of the temperature distribution of SnAgCu solder between PZT-plates; b) Evaluation of layer thickness which exceeds the Curie temperature at different initial temperatures of the solder

The low heat conduction of the piezoceramic and fast cooling of the nitrogen jet from the nozzle result in a layer thickness small enough to depolarize a negligibly thin area of the piezoceramic rods and thus full functionality of the final module is expected after generation of the conductive circuit.

4. Conclusion and outlook

The present work is focused on the fast and flexible generation of conductive circuits for electronic, optoelectronic and mechatronic devices. Thereby three different laser-based approaches are discussed. Additionally the latest results of laser-based soldering of piezo-composites are shown.

In this paper the feasibility of the generation of dense and highly conducting ITO layers starting from nanoparticle suspensions and subsequent laser consolidation in ambient air for different particle layer thicknesses is shown. Maximum conductivities of over 140 S/cm were achieved, while thinner layers displayed a higher total conductivity in comparison to thicker layers. Being a non-vacuum technology the presented approach is a promising alternative for the generation of metal oxide layers in the mass production of optoelectronic devices such as solar cells or displays. In combination with a printing process it is compatible with modern production technologies like roll-to-roll processing.

In contrast to the current MID-technology which is highly time-consuming and expensive because of the need of shape forming tools the use of additive manufacturing is a fast and flexible method for fabricating complex 3D parts. To realize functional prototypes for MID applications in this paper stereolithography and ADDIMID technology are combined. Therefore SLA resin was doped with aluminum and parts are fabricated. Afterwards the aluminum doped parts are laser-structured and chemical metalized. The analysis of the experiments showed that a selective metallization with a high conductivity and a good adhesion to the substrate can be realized. By means of condensation soldering electronic components were mounted on the metalized substrate and characterized before as well as after climate tests. It could be shown that the conductivity of the conductive circuit is nearly constant before and after the temperature shock tests whereas the shear forces to remove the electrical component decrease by means of aging. All in all the demonstrate process chain is a suitable solution for functional MID prototypes during concept stage.

Referring to the experiments presented in section 3.3, it is theoretically possible to generate simple conductive structures on sheet metals coated with a thin PA12 layer without destroying the plastic layer by laser-based additive manufacturing technologies such as LBM. Hereby a convenient process strategy and the right process parameters have to be applied. However, for the controlled and reproducible fabrication of additively generated conductive paths - not to mention more complex two- and three dimensional electronic structures of high current load capacity - further fundamental research will be required. To improve the reproducibility, the strength of substrate bonding and the electrical conductivity the applied process strategy has to be refined in order to make this approach interesting for industrial applications. Hence in the near future one of our focus areas will be the development of a novel laser-based process for the direct and fast fabrication of conductive structures of varying dimensions on different insulating materials e.g. high-temperature-resistant plastics or ceramics. Within the scope of future research even the principle of laser metal depositon (LMD) should be investigated for the fabrication of conductive structures with adequate current load capacity.

Conductive circuits of high performance transducers can preferably be generated by soldering which provides also a sufficient mechanical connection for a subsequent assembling process. Laser soldering shows small heat affected zones and enables fast processing for a mass production of the demonstrated piezoelectric modules.

Acknowledgments and Appendixes

The authors gratefully acknowledge funding of the Erlangen Graduate School in Advanced Optical Technologies (SAOT) by the German Research Foundation (DFG) in the framework of the German excellence initiative.

The support of the German Research Foundation (DFG, Graduiertenkolleg 1161/2) is gratefully acknowledged. Additionally, we are thankful for the support of by Evonik Industries AG.

The work presented in this paper focuses the research project 3A-3D-MID. The project is funded by the BMWi (Federal Ministry of Economics and Technology) and supplemental by the AiF (German Federation of Industrial Research Associations). The authors would like to thank the project committee consisting of 10 companies. The authors are deeply grateful for this support and are responsible for the contents of this publication.

This research is supported by the Deutsche Forschungsgemeinschaft (DFG) in context of the Collaborative Research Centre/Transregio 39 PT-PIESA, subproject A4.

References

[1] M. Baum, I. Alexeev, M. Schmidt: Laser Treatment of ITO and ZnO Nanoparticles for the Production of Thin Conducting Layers on Transparent Substrates, Journal of Laser Micro / Nanoengineering, 6, 191-194 (2012).

[2] M. Baum, S. Polster, M. Jank, I. Alexeev, L. Frey, M. Schmidt: Efficient laser induced consolidation of nanoparticulate ZnO thin films with reduced thermal budget, Applied Physics A - Materials Science and Processing, 107, 269-273 (2012).

[3] G. Eßer: Laserstrahlunterstützte Erzeugung metallischer Leiterstrukturen auf Thermoplastsubstraten für die MID-Technik, Dissertation, Erlangen, 2002.

[4] G. Eßer, Jahrsdoerfer, B., Urmoneit, U.; Laser-assisted fabrication of electronic circuits using the ADDIMID process. Proc. SPIE 4274, Laser Applications in Microelectronic and Optoelectronic Manufacturing VI, 375 (June 29, 2001).

[5] P. Amend, C. Pscherer, T. Rechtenwald, T. Frick, M. Schmidt: A fast and flexible method for manufacturing 3D molded interconnect devices by the use of a rapid prototyping technology, Physics Procedia, 5, Part B, 561–572 (2010).

[6] M. Mahajeri, A. Schneider, M. Baum, T. Rechtenwald, M. Voigt, M. Schmidt, W. Peukert: Production of dispersions with small particle size from commercial indium tin oxide powder for the deposition of highly conductive and transparent films, Thin Solid Films 520, 5741 (2012).

[7] J. Franke: Integrierte Entwicklung neuer Produkt- und Produktionstechnologien für räumliche spritzgegossene Schaltungsträger (3-D MID), Dissertation, Erlangen, 1995.

[8] F. Schüßler, K. Feldmann, H. Kück, H. Richter, T. Osswald, A. Gardocki: Molded Interconnect Devices for Applications with Advanced Thermal Requirements, Proceedings of the 8th international congress molded interconnect devices, Fürth, 2008.

[9] C. Pscherer, T. Frick, B. Wendel: Hohe Flexibilität bei MID Anwendungen durch den Einsatz von Rapid Prototyping Verfahren. In: M. Schmidt (ed.), M. Geiger, C. Kägeler, LEF 2009 - Laser in der Elektronikproduktion & Feinwerktechnik, Meisenbach, Erlangen, 2003,

[10] N.N.: Forschungsvereinigung Räumliche Elektronische Baugruppen 3D MID e.V. (ed.), Technologie 3D-MID, Hanser, Munich, 2004.

[11] P.F. Jacobs, D. T. Reid: Rapid prototyping & manufacturing: Fundamentals of stereolithography, Society of Manufacturing Engineers, 1992

[12] http://www.custompartnet.com/wu/images/rapid-prototyping/dmls.png, Access date: 17.07.2013

[13] V.F. Janas, A. Safari: Overview of fine-scale piezoelectric ceramic/polymer composite processing. J American Ceramic Society 78 (11), 1995, p. 2945-2955

[14] A. Schönecker, S. Gebhardt: Microsystems Technologies for Use in Structures and Integrated Systems, Advances in Science and Technology, Vol. 56, 2008, pp 76-83.

[15] R. Neugebauer, H.-J. Koriath, M. Müller: Assembly of smart adaptronic piezo-metal composites by use of prefabricated batches of piezoceramic micro parts, Proc. SPIE 8692, Sensors and Smart Structures Technologies for Civil, Mechanical, and Aerospace Systems 2013, 869224

[16] G. Legeay, X. Castel, R. Benzerga, J. Pinel: Excimer laser beam/ITO interaction: from laser processing to surface reaction. Phys. Status Solidi C 5, 3248 (2008)

[17] N.N.: Data sheet NanoTool, DSM Somos 02 (2008)

[18] M. Dittes: Elektronikweichlote für spritzgegossene Schaltungsträger, Dissertation, Bayreuth, 1999

[19] C. Kittel: Einführung in die Festkörperphysik, page 168, 14 Auflage, Oldenbourg Verlag München Wien, 2006

[20] H. Domininghaus: Kunststoffe, 8. Auflage, Springer Verlag Heidelberg, 2008

[21] U. Quentin, J. Heberle, C. Held, M. Schmidt: Laser droplet brazing for electrical contacting of composite materials with integrated active elements; Procedia Materials Science, Vol. 2, 2013, pp. 181-188

(Received: July 30, 2013, Accepted: December 3, 2013)